Quantum Information and Computation, Vol. 11, No.3&4 (2011) 0300-0312

UNIVERSAL QUANTUM COMPUTING IN LINEAR NEAREST NEIGHBOR ARCHITECTURES

PREETHIKA KUMAR and STEVEN R. SKINNER

Department of Electrical Engineering and Computer Science
Wichita, Kansas 67260, USA

Received January 28, 2009
Revised November 17, 2010

We introduce a scheme for realizing universal quantum computing in a linear nearest neighbor architecture with fixed couplings. We first show how to realize a controlled-NOT gate operation between two adjacent qubits without having to isolate the two qubits from qubits adjacent to them. The gate operation is implemented by applying two consecutive pulses of equal duration, but varying amplitudes, on the target qubit. Since only a single control parameter is required in implementing our scheme, it is very efficient. We next show how our scheme can be used to realize single qubit rotations and two-qubit controlled-unitary operations. As most proposals for solid state implementations of a quantum computer use a one-dimensional line of qubits, the schemes presented here will be extremely useful.

Key words: quantum computation, quantum architectures, linear nearest neighbour, controlled-unitary, Toffoli gate
Communicated by: B Kane & M Mosca

1 Introduction

It has been shown that in a quantum computer any multi-qubit operation can be realized using single-qubit and two-qubit controlled-NOT (CNOT) gate operations [1, 2]. Many proposed implementations for a physical quantum computer use a one-dimensional line of qubits with nearest-neighbor interactions [3-22] where each qubit interacts only with the two qubits adjacent to it. In such linear nearest-neighbor (LNN) architectures, performing a single-qubit or a CNOT gate between adjacent qubits might not be easy to implement. This is because the evolution of the qubit(s) on which the gate operation is performed depends on the states of the adjacent qubits coupled to it, making it very hard to precisely control gate operations. There are two ways of overcoming this problem – devise methods for switching couplings, or devise methods of performing computations with always-on interactions. A number of methods for isolating a qubit from its neighbors by shutting off the coupling have been devised in various quantum systems [15-28]. For instance, in phosphorus doped silicon systems, a method of applying voltage biases to surface control electrodes, in order to vary the exchange coupling between neighboring donor atoms, is employed [23]. In GaAs/AlGaAs electron spin quantum dots, the strength of the exchange interaction, which depends on the overlap of the respective electron

wavefunctions, is varied by changing the voltage applied to the gate controlling the tunnel barrier between the two dots [18]. In charge qubits, nearest neighbors are coupled via loop-shaped electrodes with Josephson junctions (JJs) at the loop intersections, where the bias currents through the coupling JJs serve as interaction control knobs [22]. In coupled quantum dot molecules, the coupling is switched off by grounding metal film electrodes between two qubits which turns off the Coulomb interaction between qubits [20]. While all these methods of switching couplings facilitate multi-qubit operations, there are disadvantages in using tunable coupling. The ability to switch couplings usually involves performing fast changes in the qubit parameters or using additional circuit elements, both of which increase the complexity of the experimental set-up and open the system to noise. Thus, methods of performing computations with always-on interactions can be a desirable alternative and a number of schemes have been proposed [29-37]. In [31], Zhou *et al.* devised a two-dimensional architectural scheme for universal and scalable quantum computation, where the coupling between encoded qubits are effectively turned on and off by computing in and out of carefully designed interaction free subspaces analogous to decoherence free subspaces. However, from a practical standpoint, their approach is complex in terms of the two-dimensional physical arrangement of qubits, initialization, and the steps involved in generating gates. In [32], Benjamin *et al.* showed how to perform computations along a one-dimensional array by tuning the Zeeman transition energies of individual qubits. However, the scheme requires placing intervening qubits in definite classical states in order to negate the residual Ising interaction, thereby increasing the computational overhead. Recently, schemes employing global control have been proposed [33, 34] and implemented in optical systems [35] and antiferromagnetic spin rings [36].

In this paper, we present a new scheme for implementing single- and two-qubit gate operations in an LNN architecture without having to shut off the coupling between adjacent qubits. Unlike previous schemes [31, 32], our method does not require encoding physical qubits into logical qubits. Neither does it require separating qubit-bearing spins by passive "barrier" spins [33], thereby significantly minimizing the computational overhead. We first describe how to implement a CNOT gate operation between two adjacent qubits where the gate operation is realized by *applying only two pulses* on the target qubit. The pulses are of equal duration, but varying amplitudes. We also show how to implement arbitrary single-qubit operations and controlled-unitary operations. Even though we use a linear array coupled through Ising interactions, our method is also relevant to a system coupled through Heisenberg interactions. Compared to previous schemes, our method is simple and efficient because only a single control parameter is required. All gate operations are achieved by varying this control parameter, with the number of pulses varying from one for the Toffoli gate, two for controlled-unitary operations like the CNOT, and four for single qubit operations.

2 Controlled-NOT Gate

Figure 1 shows a LNN architecture, where each qubit is represented as a circle. The coupling between qubits is represented by solid lines, wherein a qubit is coupled only to the two qubits adjacent to it. In our design, we assume only two coupling constants, ξ_1 and ξ_2, which alternate along the length of the architecture. The design can be implemented in systems with and without the ability to switch couplings. For instance, in charge qubits with fixed couplings [38], the coupling capacitances between adjacent boxes can be fabricated to alternate along a line of qubits. If the coupling is tunable, as in [22]

where nearest-neighbor charge qubits are coupled through loop-shaped electrodes with JJs at the loop intersections, the bias currents through alternate JJs can be fixed such that they alternate along the length of the chain. These currents, once set, will not be varied during the computation.

Consider any three adjacent qubits along the line – qubits A, B and C in Fig. 1. Suppose we wish to perform a CNOT gate operation between qubits A and B, shown in Fig 2(a), with qubit B as the target and qubit A as the control. Qubit C behaves as a "dummy" qubit. Since B is also coupled to C, this operation can only be implemented by using the equivalent circuit shown in Fig. 2(b). The reason the two couplings, ξ_1 and ξ_2, are required is so that qubit B can distinguish between qubit A, the control, and C, the "dummy". Observe that both gate operations of Fig. 2(b) are controlled-controlled-unitary operations, where the second gate is a Toffoli gate. To achieve the equivalent gate, two consecutive control pulses of equal duration, but different amplitudes, are applied on the target qubit, B. For instance, with Josephson junction qubits, since the bias acing on individual qubits is relatively easy to control, the pulses for the CNOT gate operation would constitute varying the bias acting on the target qubit. Details of calculating the magnitude of the pulses will be discussed shortly.

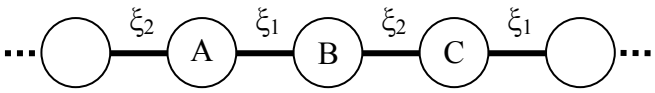

Fig. 1. Linear nearest-neighbor array of qubits where each qubit is coupled only to the two qubits adjacent to it. Here, the circles represent individual qubits and the solid lines represent the coupling between qubits. There are two coupling constants, ξ_1 and ξ_2, which alternate along the length of the chain.

Since only nearest neighbor interactions are considered [3-22], in describing the evolution of the target qubit B under a CNOT gate operation, we need only consider a Hamiltonian describing the system of qubits A, B and C, given as:

$$\mathbf{H} = \sum_{i=A,B,C} \left(\Delta \boldsymbol{\sigma}_{\mathbf{X_i}} + k \boldsymbol{\sigma}_{\mathbf{Y_i}} + \varepsilon_i \boldsymbol{\sigma}_{\mathbf{Z_i}} \right) + \xi_1 \boldsymbol{\sigma}_{\mathbf{Z_A}} \boldsymbol{\sigma}_{\mathbf{Z_B}} + \xi_2 \boldsymbol{\sigma}_{\mathbf{Z_B}} \boldsymbol{\sigma}_{\mathbf{Z_C}} \tag{1}$$

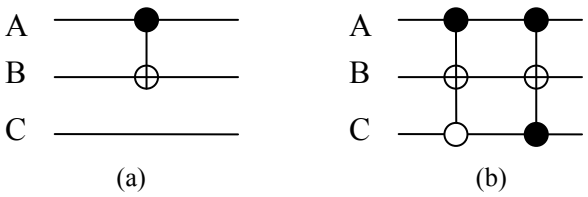

Fig. 2. Circuit (a) and equivalent circuit (b) for implementing a CNOT gate operation between qubit A and B with A as the control and B as the target.

The summation term corresponds to the Hamiltonians of each of the three qubits where Δ and k are the tunneling parameters of a qubit, and ε_i are the biases acting on individual qubits. The 8×8 matrices, $\boldsymbol{\sigma}_{\mathbf{X_i}}$, $\boldsymbol{\sigma}_{\mathbf{Y_i}}$ and $\boldsymbol{\sigma}_{\mathbf{Z_i}}$, are the Pauli spin matrices for each qubit. Throughout this paper we will use terminology specific to Josephson junction qubits. We are assuming that the qubits are identical in that

they have the same tunneling parameters. The interaction assumed between the qubits is of the Ising type, which is typical of Josephson junction qubits.

In previous work, we have shown a method for reducing the 8 × 8 matrix given by Eq. (1) to a 2 × 2 matrix describing the evolution of the target qubit B only [39, 40]. This is achieved by maintaining high biases on qubits A and C, which forces these qubits to remain in their states. The reduced Hamiltonian for the target qubit will be:

$$\mathbf{H} = \Delta\boldsymbol{\sigma}_{\mathbf{X}} + k\boldsymbol{\sigma}_{\mathbf{Y}} + \left(\varepsilon_B \pm \xi_1 \pm \xi_2\right)\boldsymbol{\sigma}_{\mathbf{Z}} \tag{2}$$

Here, the coupling terms ξ_1 and ξ_2 either add or subtract from the bias term ε_B depending on whether qubits A and C are in the $|0\rangle$ or $|1\rangle$ states, respectively [39]. This is because the expectation value of the $\boldsymbol{\sigma}_{\mathbf{Z_A}}$ ($\boldsymbol{\sigma}_{\mathbf{Z_C}}$) operator in the subspace of qubit B is either +1 or −1 depending on whether qubit A (C) is in the $|0\rangle$ or $|1\rangle$ states, respectively. Therefore, it is mandatory to choose these couplings to be different to *distinguish* between the two qubits. Observing Eq. (2), there are four different Hamiltonians governing the evolution of qubit B corresponding to the four subspaces where the states of qubits A and C are $|00\rangle$, $|01\rangle$, $|10\rangle$ and $|11\rangle$. At any instant of time, the evolution of qubit B is governed by the following 2 × 2 unitary matrix:

$$\mathbf{U} = \begin{pmatrix} \cos(2\pi ft) - i\dfrac{\mathrm{E}}{f}\sin(2\pi ft) & \dfrac{k - i\Delta}{f}\sin(2\pi ft) \\ \dfrac{-k - i\Delta}{f}\sin(2\pi ft) & \cos(2\pi ft) + i\dfrac{E}{f}\sin(2\pi ft) \end{pmatrix} \tag{3}$$

where

$$f = \sqrt{\Delta^2 + k^2 + \mathrm{E}^2} \tag{4}$$

and

$$E = \varepsilon_B \pm \xi_1 \pm \xi_2 \tag{5}$$

Here, f is the frequency of oscillation and E is the effective bias acting on the target qubit B depending on the subspace that qubit B evolves in. Note that since there are four different effective biases acting on the target qubit, there will be four different unitary matrices of the form of Eq. (3), governing the evolution of qubit B in the four corresponding subspaces. Therefore, there will be four different frequencies of oscillation (Eq. (4)).

Referring to Fig. 2(b), consider the first gate operation under which a NOT gate operation is performed on qubit B only when qubits A and C are in the $|1\rangle$ and $|0\rangle$ states, respectively. Suppose T is the time step within which the first gate operation is realized. Then, choosing k as zero (which is the case for Josephson junction qubits), since the effective bias, E, acting on the target qubit B is "$\varepsilon_B - \xi_1 + \xi_2$", the following conditions need to be satisfied in order to realize a NOT gate operation:

$$\varepsilon_B = \xi_1 - \xi_2 \tag{6}$$

$$\sqrt{\left(\Delta^2+\left(\varepsilon_B-\xi_1+\xi_2\right)^2\right)}=\frac{M+1/4}{T} \tag{7}$$

where M is an integer. The first condition, where the effective bias is made zero, makes the magnitude of the off-diagonal terms unity (and also causes the diagonal entries resulting from the sine terms to vanish). This is required so that there is no attenuation to the amplitude of oscillations of the probability function under a NOT gate operation [39]. The second condition is required to make the cosine terms in Eq. (3) zero.

Under the first gate operation in Fig. 2(b), for each of the cases when qubits A and C are in the $|00\rangle$, $|01\rangle$ and $|11\rangle$ states, we require the **U** matrix to correspond to the identity matrix. Therefore, considering the respective effective biases in each of these subspaces of the target qubit, the following conditions must be satisfied:

$$\sqrt{\left(\Delta^2+\left(\varepsilon_B+\xi_1+\xi_2\right)^2\right)}=\frac{P}{T} \tag{8}$$

$$\sqrt{\left(\Delta^2+\left(\varepsilon_B+\xi_1-\xi_2\right)^2\right)}=\frac{Q}{T} \tag{9}$$

$$\sqrt{\left(\Delta^2+\left(\varepsilon_B-\xi_1-\xi_2\right)^2\right)}=\frac{R}{T} \tag{10}$$

where P, Q and R are integers. Next, using condition (6) in Eqs. (7) through (10), we obtain the following equations:

$$\Delta=\frac{M+1/4}{T} \tag{11}$$

$$\sqrt{\left(\Delta^2+4\xi_1^2\right)}=\frac{P}{T} \tag{12}$$

$$\sqrt{\left(\Delta^2+4\left(\xi_1-\xi_2\right)^2\right)}=\frac{Q}{T} \tag{13}$$

$$\sqrt{\left(\Delta^2+4\xi_2^2\right)}=\frac{R}{T} \tag{14}$$

Next, we show that to realize the second gate operation in Fig. 2(b), the Toffoli gate, *the same values for the fixed parameters*, Δ, ξ_1 *and* ξ_2, *are used*, which were used to realize the first gate operation. This is an important condition to be realized for a practical implementation of the gate operation since, in our design, the tunneling and coupling parameters are assumed to be fixed during fabrication. The only difference is that the bias on the target qubit B will now be pulsed to a different

value. In this case, we need to perform a NOT gate operation when both qubits A and C are in the $|1\rangle$ state. The effective bias, E, acting on qubit B in this subspace is "$\varepsilon_B - \xi_1 - \xi_2$". Therefore, under the second gate operation the bias on qubit B will be pulsed to:

$$\varepsilon_B = \xi_1 + \xi_2 \tag{15}$$

Under the bias pulse given by Eq. (15), the frequencies of oscillation in the subspaces where qubits A and C are in the $|01\rangle$, $|10\rangle$, and $|11\rangle$ states are given by Eqs. (12), (14), and (11), respectively, and in the subspace where qubits A and C are in the $|00\rangle$ state is given by:

$$\sqrt{\left(\Delta^2 + 4\left(\xi_1 + \xi_2\right)^2\right)} = \frac{S}{T} \tag{16}$$

The set of equations (11) through (14) and Eq. (16) are next solved for different values of M, P, Q, R and S, to obtain the parameters of the system. Observe that by choosing ξ_1 to be twice as much as ξ_2, Eq. (13) reduces to the same equation as Eq. (14). One set of values for Δ, ξ_1 and ξ_2 are 25MHz, 400MHz and 200MHz, respectively (for M=0, P=8, Q=4, R=4 and S=12), using a time step T of 10 ns. Subject to these calculated parameters, to realize a CNOT gate operation between qubits A and B, the bias on the target qubit B is first pulsed from a from a high value (typically 10GHz in our simulations) to a value of 200 MHz for a duration of 10 ns, after which it is increased to 600MHz for 10ns. At the end of the gate operations, the bias on the target qubit is once again made high.

An important feature of the pulsed bias scheme is that the parameters can be scaled, where the limits on the parameter values are those imposed by experimental conditions. This means that having found the parameter values for a pulse width of certain duration, the parameters for a different pulse width are just a multiple of the original values (the multiple depends on the ratio of the two pulse widths under consideration). Therefore, our method can be implemented in most practical schemes [41]. For instance, the calculated values of the parameters in the previous paragraph are realistic for superconducting flux qubits [42]. For charge qubits, picosecond pulses are applied and the values of the parameters vary in the GHz range [38]. Therefore, the same parameters to implement gate operations in charge qubits would be: Δ=25GHz, ξ_1=400GHz, ξ_2=200GHz, and T=10ps. Similarly, for ion trap computers, the parameters will be in the KHz range and time pulses will be in the microseconds range [43].

Observing the unitary matrix given by Eq. (3), it is important to point that the NOT gate operation is realized with a global phase of "$\pm\pi/2$". Therefore, for the chosen parameters, the CNOT gate operation between qubits A and B corresponds to the following operator (we have ignored the state of the "dummy" qubit C):

$$|00\rangle\langle 00| + |01\rangle\langle 01| - i|10\rangle\langle 11| - i|11\rangle\langle 10| \tag{17}$$

The phase factor of "–i" is overcome by applying a single qubit gate on the control qubit [1] as shown in Fig. (3). However, in section 4, we will show how phases developed as a result of the control qubits can be used to realize perfect gate operations. Note that if we had chosen Δ as zero instead of k, i.e.,

the off-diagonal "tunneling" parameter is a contribution by a $\boldsymbol{\sigma}_{\mathbf{Y}}$ component in the single-qubit Hamiltonian, the following gate operation would have been realized:

$$|00\rangle\langle 00| + |01\rangle\langle 01| + |10\rangle\langle 11| - |11\rangle\langle 10| \tag{18}$$

which corresponds to a controlled-rotation (CROT) gate [44]. By performing a controlled-Z operation after the CROT gate operation, the phase factor is removed and a CNOT gate is realized. Methods for realizing single qubit and arbitrary controlled-unitary operations are discussed in the next section.

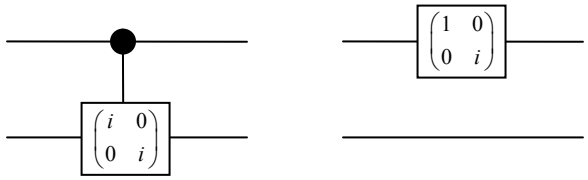

Fig. 3. (a) Controlled phase shift gate for overcoming the "-i" phase introduced by the gate in Eq. (17). (b) Equivalent circuit where a single qubit rotation is applied on the control qubit.

3 Single Qubit Rotations

Figure 4 shows three different methods for realizing single qubit gate operations on a qubit in the LNN architecture shown in Fig. 1. In Fig. 4(a), a unitary operation is implemented on qubit B, by keeping the qubits adjacent to it in the $|0\rangle$ state. This requires that some of the qubits in the LNN architecture be prepared in the $|0\rangle$ state. We refer to these $|0\rangle$ states as "isolation" states, which are moved down the LNN architecture from one qubit to another via swap operations. (Each swap operation can be decomposed into two CNOT operations). When a unitary operation is to be performed on a qubit, say B, $|0\rangle$ states are moved down the line to the qubits adjacent to it as shown in Fig. 4(a). The qubit is thus isolated from its neighbors without having to switch off its couplings. By maintaining high biases on the two adjacent qubits in the $|0\rangle$ state, the reduced Hamiltonian for qubit B is:

$$\mathbf{H} = \Delta\boldsymbol{\sigma}_{\mathbf{X}} + k\boldsymbol{\sigma}_{\mathbf{Y}} + \left(\varepsilon_B + \xi_1 + \xi_2\right)\boldsymbol{\sigma}_{\mathbf{Z}} \tag{19}$$

As seen by the Hamiltonian, qubit B can now be treated as a single qubit system with an effective bias "$\varepsilon_B+\xi_1+\xi_2$" acting on it (instead of bias "ε_B" for an isolated single qubit system). After the desired gate operation is achieved, the isolation qubits can be moved away again.

Figure 4(b) shows how to implement a single qubit operation on qubit B, treating only qubit C as an isolation qubit. In this case, the reduced Hamiltonian for qubit B is:

$$\mathbf{H} = \Delta\boldsymbol{\sigma}_{\mathbf{X}} + k\boldsymbol{\sigma}_{\mathbf{Y}} + \left(\varepsilon_B \pm \xi_1 + \xi_2\right)\boldsymbol{\sigma}_{\mathbf{Z}} \tag{20}$$

Since there are two different effective biases "$\varepsilon_B - \xi_1 + \xi_2$" and "$\varepsilon_B + \xi_1 + \xi_2$" acting on the target qubit, two pulses of equal duration, but different magnitudes, are required to achieve the gate operation. In [40], we have shown how to compute the magnitude of the first pulse. Finding the magnitude of the second pulse is straightforward. For instance, under a controlled-Hadamard gate, the magnitude of the two pulses will be "$\varepsilon_B = \Delta + \xi_1 - \xi_2$" and "$\varepsilon_B = \Delta + \xi_1 + \xi_2$", respectively.

Figure 4(c) shows how a unitary gate operation can be realized without having to move $|0\rangle$ states to qubits A and C. The operation requires four pulses. For a NOT gate, the values of these pulses are: "$\varepsilon_B = -\xi_1 - \xi_2$"; "$\varepsilon_B = -\xi_1 + \xi_2$"; "$\varepsilon_B = \xi_1 - \xi_2$" and "$\varepsilon_B = \xi_1 + \xi_2$". The values of the parameters ε_B, ξ_1 and ξ_2 are the same as that calculated in section 2 for the CNOT gate. Calculating the parameters for other unitary transformations, like the Hadamard gate, is not straightforward and requires numerical simulations.

Arbitrary two-qubit controlled-unitary gates can be realized by circuits similar to Figs. 4(b) and 4(c). In using Fig. 4(b), the second gate operation is not performed. Similarly, in using Fig. 4(c), the first two gate operations are not performed. Details of calculating parameters for realizing arbitrary controlled-unitary operations in two-qubit systems have been presented elsewhere [40].

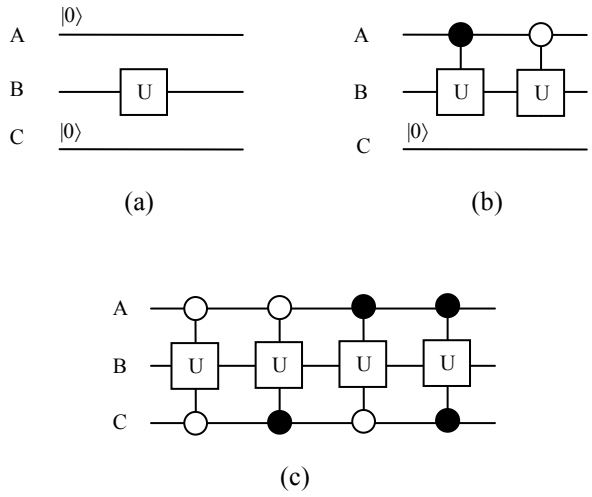

Fig. 4. Three methods for realizing a unitary operation on a single qubit (B) using our LNN architecture. (a) Qubits A and C function as isolation qubits. The gate operation is realized in a single pulse. (b) Qubit C functions as an isolation qubit. The gate operation is realized in two pulses. (c) The gate operation is realized in four pulses, each of which corresponds to a controlled-controlled gate operation.

When qubits are idle and no gate operations are performed on them, relative phases develop as a result of qubit precessions. However, by perfectly timing the time interval between gate operations such that these phases evaluate to an even integer multiple of 2π, these phases can be overcome or minimized. Another method would be to implement a scheme similar to [45], where qubits in definite spin states can be used to separate qubits in arbitrary quantum states. However, even though placing intervening qubits in definite spin states negates the Ising interaction, this method increases the computational overhead. This is because to perform a two-qubit gate operation between two qubits in

arbitrary states in the array, additional swap operations are required to bring the qubits together. Phases also develop as a result of precessions of the control qubits during gate operations, and due to the effect of finite rise and fall times in the applied bias pulses. In the next two sections, the effects of these phases on gate operations will be investigated.

It is important to point that while we have restricted our discussion to LNN architectures where the qubits are coupled via Ising interactions, the method presented here easily extends to systems coupled via Heisenberg interactions. This is because if the difference in the magnitudes of the biases on neighboring qubits is much greater than the coupling strengths, the Heisenberg interaction becomes Ising [46]. Since, in our scheme, the bias on the target qubit is always pulsed to a different value (of the order of the coupling) than the applied bias on neighboring qubits, the interaction will always be of the Ising type.

4 Relative Phases on Gate Operations Due to the Presence of Control Qubits

As discussed in section 3, in implementing a CNOT gate between qubits A and B, the biases on the control (ε_A) and dummy qubits (ε_C) are maintained high throughout, while the bias on the target qubit (ε_B) is pulsed from a high value to a low calculated value for time step T. As a result, relative phases develop between the basis states. In the subspaces where qubits A and C are in the $|00\rangle$, $|01\rangle$, $|10\rangle$ and $|11\rangle$ states, the relative phases developed between the $|0\rangle$ and $|1\rangle$ states of qubit B are $\exp(i(\varepsilon_A+\varepsilon_C)T)$, $\exp(i(\varepsilon_A-\varepsilon_C)T)$, $\exp(i(-\varepsilon_A+\varepsilon_C)T)$, $\exp(i(-\varepsilon_A-\varepsilon_C)T)$, respectively. Previously, the high value of biases ε_A and ε_C were so chosen such that each of these phases evaluated to zero or an even integer multiple of 2π. However, *instead of cancelling out these phases, the phases can be used to obtain "perfect" gate operations*. In most systems, gate operations themselves are not realized perfectly, due to the structure of the internal Hamiltonian. For instance, in the system described by Eq. (1) with k as zero, a CNOT gate operation is realized with a relative phase between the basis states as given by Eq. (17). This is because a NOT gate can only be realized up to an overall global phase of $\pm\pi/2$. Therefore, if the phases from the control qubits can be used to cancel out this $\pi/2$ phase, a perfect gate operation can be realized.

Taking into account the relative phases due to the two control qubits, the gate operations realized under the first and second pulses in Fig. 2(b) now become:

$$\begin{aligned}\mathbf{G_1} = {} & e^{i2\pi(\varepsilon_A+\varepsilon_C)T}\left(|000\rangle\langle 000|+|010\rangle\langle 010|\right)+e^{i2\pi(\varepsilon_A-\varepsilon_C)T}\left(|001\rangle\langle 001|+|011\rangle\langle 011|\right)\\ & -ie^{i2\pi(-\varepsilon_A+\varepsilon_C)T}\left(|100\rangle\langle 110|+|110\rangle\langle 100|\right)+e^{i2\pi(-\varepsilon_A-\varepsilon_C)T}\left(|101\rangle\langle 101|+|111\rangle\langle 111|\right)\end{aligned} \tag{21}$$

$$\begin{aligned}\mathbf{G_2} = {} & e^{i2\pi(\varepsilon_A+\varepsilon_C)T}\left(|000\rangle\langle 000|+|010\rangle\langle 010|\right)+e^{i2\pi(\varepsilon_A-\varepsilon_C)T}\left(|001\rangle\langle 001|+|011\rangle\langle 011|\right)\\ & +e^{i2\pi(-\varepsilon_A+\varepsilon_C)T}\left(|100\rangle\langle 100|+|110\rangle\langle 110|\right)-ie^{i2\pi(-\varepsilon_A-\varepsilon_C)T}\left(|101\rangle\langle 111|+|111\rangle\langle 101|\right)\end{aligned} \tag{22}$$

Choosing $\varepsilon_A = -\varepsilon_C$ under gate operation $\mathbf{G_1}$ and $\varepsilon_A = \varepsilon_C$ under gate operation $\mathbf{G_2}$, we have

$$\begin{aligned}\mathbf{G_2 \cdot G_1} = e^{i2\pi(2\varepsilon_A)T}\left(|000\rangle\langle 000| + |010\rangle\langle 010| + |001\rangle\langle 001| + |011\rangle\langle 011|\right) \\ -ie^{i2\pi(-2\varepsilon_A)T}\left(|100\rangle\langle 110| + |110\rangle\langle 100| + |101\rangle\langle 111| + |111\rangle\langle 101|\right)\end{aligned} \tag{23}$$

Suppose δ is a slight adjustment to ε_A, i.e., $\varepsilon_A = \varepsilon_A' + \delta$, where ε_A' is the originally chosen high value of the bias (10GHz in simulations). Next, by choosing δ such that $\exp(i(-2\pi(4\delta)T)$ is "+i", the CNOT gate is perfectly realized up to an overall global phase of $\exp(i4\pi\delta T)$. The minimum value of δ is 6.25MHz. Depending upon the resolution which the physical quantum system under consideration allows, higher values of δ can be obtained by evaluating the phase to be higher odd-integer multiples of $\pi/2$.

5 Effects of Finite Rise and Fall Times on the Performance of Gate Operations

Even though we use ideal pulses in our simulations, this is not typically the case in an experimental system where pulses are non-ideal with finite rise and fall times. As a result, the switching process itself might give rise to non-ideal gate operations which needs to be investigated. To study these effects, simulations were carried out for the Toffoli gate (pulse 2 of the CNOT gate operation) under different rise (T_R) and fall (T_F) times. Figure 5 shows the bias pulse on the target qubit under a non-ideal pulse.

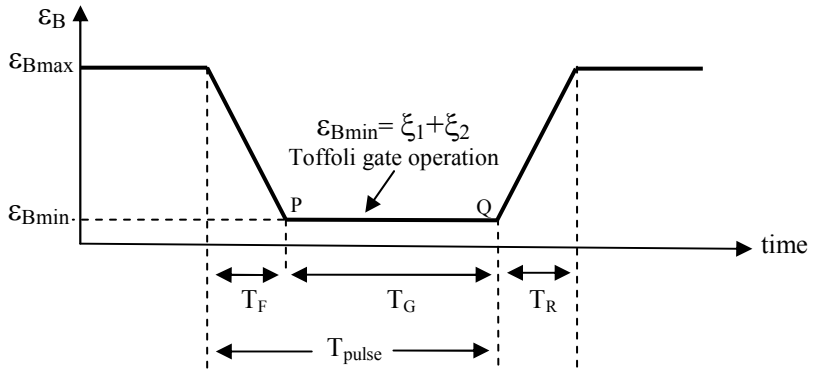

Fig. 5. Bias pulse on the target qubit, B, during a Toffoli gate operation on a three-qubit system. The bias is pulsed from a high value, ε_{Bmax}, to a low value, $\varepsilon_{Bmin} = \xi_1 + \xi_2$.

For an ideal bias pulse on the target qubit (T_F=T_R=0), the pulse width "T" is as that calculated in section 2 (Eq. (11)). However, simulation results show that, under a non-ideal pulse, to increase the fidelity of a Toffoli gate, the time for which the bias is held at ε_{Bmin} has to be reduced (T_G=T−T_C). This is because near points P and Q, the value of the bias, ε_B, becomes comparable with ε_{Bmin} (600MHz). This causes the *magnitudes* of the probability amplitudes in the state vector to change, which affects the overall gate operation. Therefore, the pulse width for the gate operation is recalculated as follows:

$$T_{pulse} = T_G + T_F = \left(T - T_C\right) + T_F \tag{24}$$

where
$$T_C = \sqrt{\frac{T_{AVG}}{2(\delta\varepsilon_B)}} = \frac{1}{2}\sqrt{\frac{T_R + T_F}{(\varepsilon_{B\max} - \varepsilon_{B\min})}} \tag{25}$$

Here, T_{pulse} is the pulse time, $\delta\varepsilon_B$=(ε_{Bmax}−ε_{Bmin}) is the difference between the maximum and minimum bias, and T_{AVG} is the average of the rise and fall times. The correction factor, T_C, depends on the *average slope* (magnitudes only) of the rise and fall lines. This means that for a given value of $\delta\varepsilon_B$ and T_{AVG}, the gate performance was identical whether or not T_F and T_R were equal. It was also found that the expression for the correction factor T_C depends on the product "$T{\cdot}\Delta$" as given by Eq. (11). Equation (25) corresponds to an expression for T_C when M is zero ($T{\cdot}\Delta$ is 0.25). A new expression would need to be derived for different values of M. However, for larger values of M, the fidelity of the gate operation itself decreases, and therefore, the best gate performance under a non-ideal pulse is when M is zero. It is important to point that even though Eq. (25) was derived with the Toffoli gate as the gate operation, the same equation can be used for the first pulse in Fig. 2(b). In other words, as long as the average slope, $\delta\varepsilon_B/T_{AVG}$, is the same for both pulses, the value of T_C is the same for both gate operations.

At other points along the rise/fall lines (not in the vicinity of P and Q), only the relative phases between the basis states change, with no change in the magnitudes of the amplitudes. The values of these phases are completely random, depending both on the slope of the lines and the resolution of the time step used in simulation. Calculating the exact value of these phases analytically, is out of the scope of this paper. However, it was found that for a given value of $\delta\varepsilon_B$, the relative phases in the final state do not vary with the slope of the rise/fall lines.

Following were the conclusions drawn from this analysis: (a) The effect of finite rise/fall times on gate operations depends on the slope of the rise/fall lines; (b) A steep slope (1-10 GHz/ns) did not cause much change in the overall probabilities, and the effect of the rise/fall times was equivalent to a Z-rotation before and after the gate operation; (c) A gradual slope (lower than 1 GHz/ns) causes non-ideal gate operations where the magnitudes of the probability amplitudes change; (d) The effects of these non-ideal gate operations can be minimized by adjusting the gate time to an optimal value, T_G, depending on the slope of the rise/fall lines (Eq. (24)); (e) The value of T_G for a given slope ($\delta\varepsilon_B/T_{AVG}$) is the same irrespective of the value of ε_{Bmax} and ε_{Bmin}, i.e., for both pulses in Fig. 2(b), as long as the average slope, $\delta\varepsilon_B/T_{AVG}$, is the same, the value of T_C for either pulse is calculated using Eq. (25).

5 Conclusions

In this paper, we have presented a scheme for implementing universal quantum computation in LNN architectures without having to switch the coupling. The scheme is general and can be can be extended towards any two-level system whose Hamiltonian can be reduced to that of a spin boson. Even though we use a linear array coupled through Ising interactions, our method is also relevant to a system coupled through Heisenberg interactions. We first showed how to implement a CNOT gate operation between two adjacent qubits, where the gate operation is realized by *applying only two pulses* of equal duration, but varying amplitudes, on the target qubit. We next showed how to implement arbitrary single-qubit operations and controlled-unitary operations. The advantage of this scheme is that it is

simple and efficient because only a single control parameter is required. Moreover, unlike some other methods, ours does not require encoding physical qubits into logical qubits, thereby, significantly minimizing the computational overhead.

References

1. M. A. Nielson and I. L. Chuang, *Quantum computation and quantum information* (Cambridge University Press, Cambridge, England, 2001).
2. A. Barenco, *et al.*, Phys. Rev. A 52, 3457 (1995).
3. B. E. Kane, Nature (London) 393, 133 (1998).
4. A. J. Skinner, M. E. Davenport and B. E. Kane, Phys. Rev. Lett., 90, 087901 (2003).
5. L. C. L. Hollenberg, A. S. Dzurak, C. Wellard, A. R. Hamilton, D. J. Reilly, G. J. Milburn, and R. G. Clark, Phys. Rev. B 69, 113301 (2004).
6. K. Yang *et. al*, Chinese Phys. Lett 20, 991 (2003).
7. J. K. Pachos and P. L. Knight, Phys. Rev. Lett. 91, 107902 (2003).
8. M. Friesen, P. Rugheimer, D. E. Savage, M. G. Lagally, D. W. van der Weide, R. Joynt and M. A. Eriksson, Phys. Rev. B 67, 121301(R) (2003).
9. P. Solinas, P. Zanardi, N. Zanghi and F. Rossi, Phys. Rev. B 67, 121307(R) (2003).
10. J. H. Jefferson, M. Fearn and D. L. J. Tipton, Phys. Rev. A 66, 042328 (2002).
11. V. N. Golovach and D. Loss, Semicond. Sci. Tech. 17, 355 (2002).
12. T. D. Ladd, J. R. Goldman, F. Yamaguchi and Y. Yamamoto, Phys. Rev. Lett. 89, 017901 (2002).
13. E. O. Kamenetskii and O. Voskoboynikov, condmat/0310558 (2003).
14. B. Golding and M. I. Dykman, cond-mat/0309147 (2003).
15. E. Novais and A. H. Castro Neto, Phys. Rev. A 69, 062312 (2004).
16. R. Vrijen, E. Yablonovitch, K. Wang, H. W. Jiang, A. Balandin, V. Roychowdhury, T. Mor and D. DiVincenzo, Phys. Rev. A 62, 012306 (2000).
17. L. Tian and P. Zoller, Phys. Rev. A 68, 042321 (2003).
18. L. M. K. Vandersypen, R. Hanson, L. H. W. van Beveren, J. M. Elzerman, J. S. Greidanus, S. D. Franceschi, and L. P. Kouwenhoven, in Quantum Computing and Quantum Bits in Mesoscopic Systems, edited by A. J. Leggett, B. Ruggiero, and P. Silvestrini (Kluwer Academic/Plenum Publishers, New York, 2003).
19. V. V'yurkov and L. Y. Gorelik, Quant. Comput. And Comput. 1, 77 (2000).
20. N.-J.Wu, M. Kamada, A. Natori, and H. Yasunaga, Jpn. J. Appl. Phys. 39, 4642 (2000).
21. S. H. W. van der Ploeg *et al*., Phys. Rev. Lett. 98, 0507004 (2007).
22. J. Lantz, M. Wallquist, V. S. Shumeiko, and G. Wendin, Phys. Rev. B 70, 140507 (2004).
23. C.J. Weller, L.C.L. Hollenberg, L.M. Kettle, and H-S Goan, J. Phys.: Condens. Matter, 16, No. 32, 5697 (2004).
24. E.A. Stinaff, *et al.*, Science 311, 636 (2006).
25. S. Ashhab, and F. Neri, Phys. Rev. B 76, 132513 (2007).
26. A.O. Niskanen, *et al.*, Science 316, 723 (2007).
27. D.P. DiVincenzo, G. Burkard, D. Loss, and E.V. Sukhorukov, in *Quantum Mesoscopic Phenomena and Mesoscopic Devices in Microelectronics*, edited by I.O. Kulik and R. Ellialtoglu (NATO ASI, Turkey, June 13-25, 1999); cond-mat/99112445.
28. D.P. DiVincenzo, D. Bacon, J. Kempe, G. Burkard, and K.B. Whaley, Nature 408, 339 (2000).
29. G.P. Berman, G.D. Doolen, and V.I. Tsifrinovich, Superlattices and Microstructures 27, 89 (2000).
30. G.P. Berman, G.D. Doolen, D.I. Kamenev, and V.I. Tsifrinovich, in: *Quantum Computation and Information*, Complementary Mathematics 305, 13 (2002).
31. X. Zhou, Z. Zhou, G. Guo and M. J. Feldman, Phys. Rev. Lett. 89, 197903 (2002).
32. S.C. Benjamin, and S. Bose, Phys. Rev. Lett. 90, 247901, (2003).
33. R. Raussendorf, Phys. Rev. A 72, 052301 (2005).

34. J. Fitzsimons, and J. Twamley, Phys. Rev. Lett. 97, 090502 (2006).
35. B.W. Lovett, New J. of Phys. 8, 69 (2006).
36. F. Troiani, M. Affronte, S. Carretta, P. Santini, and G. Amoretti, Phys. Rev. Lett. 94, 190501 (2004).
37. G.F. Mkrtchian, Phys. Lett. A 372, Issue 32, 5270 (2008).
38. T. Yamamoto, Y.A. Pashkin, O. Astafiev, Y. Nakamura, and J.S. Tsai, Nature 425, 941 (2003).
39. P. K. Gagnebin, *et. al*, Phys. Rev. A 72, 042311 (2005).
40. P. Kumar and S. R. Skinner, Phys. Rev A 76, 022335 (2007).
41. R.V. Meter, and M. Oskin, ACM J. Emerg. Tech. in Comp. Sys. 2, 31 (2006).
42. J.H. Platenberg, P.C.de Groot, C.J.P.M. Harmans, and J.E. Mooij, Nature 447, 836 (2007).
43. D.B. Leibfried, *et al.*,Nature 422, 412 (2003).
44. S.C. Benjamin, and S. Bose, Phys. Rev. A. 70, 032314, (2004).
45. P. Chen, C. Piermarocchi, and L. J. Sham, Phys. Rev. Lett. 87, 067401, (2001).
46. P.W. Anderson, *Concepts in Solids*, Addison Wesley (Redwood City 1963).